Opposite Effects of Src Family Kinases on YAP and ERK Activation in Pancreatic Cancer Cells: Implications for Targeted Therapy

James Sinnett-Smith[1,2], Tarique Anwar[1,3], Elaine F. Reed[3], Yaroslav Teper[4], Guido Eibl[4], and Enrique Rozengurt[1,2]

ABSTRACT

Pancreatic ductal adenocarcinoma (PDAC) remains an aggressive disease that is expected to become the second cause of cancer fatalities during the next decade. As therapeutic options are limited, novel targets, and agents for therapeutic intervention are urgently needed. Previously, we identified potent positive crosstalk between insulin/IGF-1 receptors and G protein–coupled (GPCR) signaling systems leading to mitogenic signaling in PDAC cells. Here, we show that a combination of insulin and the GPCR agonist neurotensin induced rapid activation of Src family of tyrosine kinases (SFK) within PANC-1 cells, as shown by FAK phosphorylation at $Tyr^{576/577}$ and Tyr^{861}, sensitive biomarkers of SFK activity within intact cells and Src^{416} autophosphorylation. Crucially, SFKs promoted YAP nuclear localization and phosphorylation at Tyr^{357}, as shown by using the SFK inhibitors dasatinib, saracatinib, the preferential YES1 inhibitor CH6953755, siRNA-mediated knockdown of YES1, and transfection of epitogue-tagged YAP mutants in PANC-1 and Mia PaCa-2 cancer cells, models of the aggressive squamous subtype of PDAC. Surprisingly, our results also demonstrate that exposure to SFK inhibitors, including dasatinib or knockdown of YES and Src induces ERK overactivation in PDAC cells. Dasatinib-induced ERK activation was completely abolished by exposure to the FDA-approved MEK inhibitor trametinib. A combination of dasatinib and trametinib potently and synergistically inhibited colony formation by PDAC cells and suppressed the growth of Mia PaCa-2 cells xenografted into the flank of nude mice. The results provide rationale for considering a combination(s) of FDA-approved SFK (dasatinib) and MEK (e.g., trametinib) inhibitors in prospective clinical trials for the treatment of PDAC.

Introduction

One of the deadliest types of cancer has been and still is pancreatic ductal adenocarcinoma (PDAC). An estimated 48,220 patients will succumb to this disease, putting PDAC as the third leading cause of cancer mortality in the United States (1). Furthermore, PDAC is projected to become the second leading cause of cancer-related deaths before 2030 (2). Considering the failure to date to treat PDAC, there is an urgent need to identify novel targets and therapeutic agents to treat this devastating disease.

There is consensus about the importance of mutated *KRAS* (encoding KRAS) in the initiation of PDAC, occurring in >90% of human PDAC (3), a notion supported by preclinical models of the disease (4). Although a critical role of *KRAS* mutations in PDAC development is generally accepted, recent studies demonstrated that *KRAS* is dispensable for the survival of the most aggressive subtype of PDAC, that is, the squamous subtype tumors (5). Therefore, it is important to identify additional oncogenic drivers that might represent targetable vulnerabilities of the disease.

The structurally related nonreceptor Src family of tyrosine kinases (SFK) have been implicated in the regulation of cellular cytoskeletal organization, migration, and proliferation, and involved in invasion and metastasis in multiple solid tumors, including PDAC (6–8). The SFK comprises 12 members two of which, Src and YES1, are expressed prominently in human PDAC cell lines (9). An early study demonstrated that administration of the SFK inhibitor dasatinib (10) prevented metastatic dissemination in preclinical models of PDAC but did not interfere with the growth of the primary tumor (11). Subsequent clinical trials in PDAC patients using dasatinib in combination with gemcitabine (12, 13) or 5-fluorouracil and oxaliplatin (14) failed to demonstrate significant clinical benefit in patients with PDAC. The mechanism(s) leading to dasatinib resistance in PDAC are poorly understood.

Intriguingly, SFKs phosphorylate wild type and oncogenic (G12D) KRAS on tyrosine residues (Tyr^{32} and Tyr^{64}), thereby inducing conformational changes that inhibit KRAS stimulation of RAF/MEK/ERK (15, 16). Conversely, the pro-oncogenic tyrosine phosphatase SHP2 (17, 18), which dephosphorylates KRAS (19), promoted RAF/MEK/ERK signaling. Consequently, SFK-mediated tyrosine phosphorylation of KRAS in PDAC could function in a tumor-suppressive capacity via KRAS inactivation (15, 19) and thus, SFK inhibitors could induce KRAS hyper-activation.

Given the apparent inhibitory effects of SFK on KRAS-dependent signaling, we hypothesized that SFKs promote progression of PDAC acting through a downstream target(s) that circumvents the requirement of KRAS-stimulated proliferation. A plausible candidate is the transcriptional co-activator YES1-Associated Protein (YAP), a major effector of the Hippo, growth factor, G protein–coupled receptor (GPCR) and integrin signaling pathways and a key

[1]Division of Digestive Diseases, Department of Medicine, David Geffen School of Medicine, University of California, Los Angeles, California. [2]VA Greater Los Angeles Health System. [3]Department of Pathology and Laboratory Medicine, University of California, Los Angeles, California. [4]Department of Surgery, University of California, Los Angeles, California.

J. Sinnett-Smith and T. Anwar contributed equally as the co-senior authors in this article.

Corresponding Author: Enrique Rozengurt, Medicine/Division of Digestive Diseases, University of California, Los Angeles, 650 Charles E. Young Dr. S, Los Angeles, CA 90095. E-mail: erozengurt@mednet.ucla.edu

Mol Cancer Ther 2022;21:1652–62

doi: 10.1158/1535-7163.MCT-21-0964

regulator of development, organ-size, tissue regeneration, and tumorigenesis (20–22). When localized in the nucleus, YAP binds and activates predominantly the TEA-domain DNA-binding transcription factors (TEAD 1–4) thereby stimulating the expression of multiple genes. Recent evidence indicates that YAP acts as a potent oncogene in PDAC (23–25). Accordingly, YAP is overactive in PDAC tumor samples (26–28) and higher expression of YAP is correlated with poorer survival in patients with PDAC (25, 29). Importantly, YAP is highly activated in the squamous subtype of PDAC (30), which exhibits reduced dependency on KRAS for survival (31, 32). Accordingly, amplification and overexpression of *Yap* can substitute for mutant *Kras* expression in promoting PDAC in preclinical models (26). Several studies in other cell types indicated that SFKs lead to YAP activation (33–35), but the mechanisms are cell-context dependent and the role of SFKs in YAP regulation in pancreatic cancer cells has not been examined before.

In previous studies, we identified potent positive crosstalk between insulin/IGF-1 receptors and GPCR signaling systems leading to mitogenic signaling in PDAC cells (36). Subsequently, we reported that stimulation of these cells with insulin and the GPCR agonist neurotensin promoted YAP nuclear localization and activity (37). Here, we demonstrate that the SFKs play a major role in mediating YAP nuclear localization and colony growth of pancreatic PANC-1 and Mia PaCa-2 cancer cells, models of the aggressive squamous subtype of PDAC (32). Mechanistically, the SFK members YES and Src stimulate YAP phosphorylation on Tyr^{357} and the phosphorylation of this residue plays a critical role in the regulation of YAP nuclear localization. Finally, we demonstrate that exposure of PDAC cells to SFK inhibitors, including dasatinib (10), induces ERK activation and that a combination of SFK inhibitor and MEK inhibitor potently inhibited colony formation by these cells and suppressed the growth of Mia PaCa-2 cells xenografted into the flank of nude mice. The results provide rationale for considering a combination(s) of FDA-approved SFK (e.g., dasatinib) and MEK (e.g., trametinib) inhibitors in prospective trials for the treatment of PDAC.

Materials and Methods

Cell culture

PANC-1 and Mia PaCa-2 were maintained in DMEM supplemented with 10% FBS. Capan-2 were maintained in McCoy's 5A medium supplemented with 10% FBS. Human pancreatic cancer cell lines were obtained from ATCC on the following dates: PANC-1 (February 2021, April 2021, April 2022), Mia Paca-2 (February 2021, April 2021, April 2022), and Capan 2 (August 2021). These cell lines were tested for mycoplasma and authenticated by the ATCC using short-tandem repeat analysis. All cell lines were used within 15 passages after recovery from frozen stocks. No authentication or mycoplasma testing was done by the authors.

Western blot analysis

The cultures were directly lysed in 2 × SDS-PAGE sample buffer [200 mmol/L Tris-HCl (pH 6.8), 2 mmol/L EDTA, 0.1 M Na_3VO_4, 6% SDS, 10% glycerol, and 4% 2-mercaptoethanol], followed by SDS-PAGE and transfer to Immobilon-P membranes (Millipore). Membranes were blocked with 5% nonfat dried milk in PBS and then incubated overnight with the desired antibodies diluted in PBS containing 0.1% Tween. Primary antibodies bound to immunoreactive bands were visualized by enhanced chemiluminescence (ECL) detection with horseradish peroxidase-conjugated anti-mouse or anti-rabbit antibody and a FUJI LAS-4,000 mini luminescent image analyzer. Quantification of the bands was performed using the FUJI Multi Gauge V3.0 analysis program.

Immunofluorescence

Immunofluorescence of PDAC cells was performed by fixing the cultures with 4% paraformaldehyde followed by permeabilization with 0.4% Triton X-100. Cultures were then incubated for 2 hours at 25°C in blocking buffer (BB), consisting of PBS supplemented with 5% BSA, then incubated at 4°C overnight with a YAP mouse mAb (1:200) diluted in BB. Bound primary antibody was detected using Alexa Fluor 488-conjugated goat-anti mouse (1:1,000) for 1 hour at 25°C. Nuclei were stained using a Hoechst 33342 stain (1:10,000). Images were captured as uncompressed 24-bit TIFF files captured with an epifluorescence Zeiss Axioskop and a Zeiss (Achroplan 40/0.75W objective) and a cooled (−12°C) single CCD color digital camera (Pursuit, Diagnostic Instruments) driven by SPOT version 4.7 software. Alexa Fluor 488 signals were observed with a HI Q filter set 41001 and TRITC images with a HI Q filter set 41002c (Chroma Technology).

Image analysis

For YAP localization the average fluorescence intensity in the nucleus and just outside the nucleus (cytoplasm) was measured to determine the nuclear/cytoplasmic ratios. All Image analysis was performed using Zeiss analysis imaging software. The selected cells displayed in the appropriate figures were representative of 80% of the population.

siRNA and plasmid transfections

All siRNA transfection experiments were performed using Lipofectamine RNAiMAX (Life Technologies) following manufacturer's instructions. The siRNA concentration used was 10 nmol/L.

PANC-1 and Mia PaCa-2 cells were transfected with the plasmid containing a cDNA encoding FLAG-tagged YAP wild type and mutants from Addgene by using Lipofectamine 3000 (Invitrogen) as suggested by the manufacturer. Analysis of the cells transiently transfected was performed 24 hours after transfection.

Colony formation assay

For cell colony formation, 500 PANC-1, Mia PaCa-2, or Capan-2 cells were plated into 35 mm tissue culture dishes in DMEM containing 10% FBS. After 24 hours of incubation at 37°C, cultures were incubated with DMEM or McCoy's medium containing 3% FBS either in the absence or presence of tramenitib, dasatinib, or their combination. Colonies, consisting of at least 50 cells, were stained with Giemsa. Colony numbers from at least three dishes per condition were determined after 8 to 10 days of incubation and repeated in three to five independent experiments. The combination index (CI) was calculated using the equation CI = TCx/Tx + DCx/Dx, where Tx and Dx represented concentrations of trametinib (T) or dasatinib (D) added singly to produce x% inhibition, whereas TCx and DCx were the concentrations of trametinib and dasatinib in combination to elicit the same effect. CI < 1 indicated synergism.

qRT-PCR

RNA was extracted to measure gene expression. Following cDNA synthesis, real-time qPCR was performed using *CTGF*- or *CYR61*-specific primers. *CTGF* or *CYR61* mRNA expression levels were normalized to 18S mRNA levels. Data are presented as the mean of three replicates with error bars representing SEM. All reactions were performed using the Applied Biosystems StepOne system and TaqMan

Fast Advanced Master Mix. The following primers were used CTGF (Assay ID: Hs01026927_g1), CYR61 (Assay ID: Hs99999901_s1), and 18S (Assay ID: Hs99999901_s1) all were from Life Technologies.

Mice xenografts

Early passage Mia PaCa-2 cells were harvested, and 4×10^6 cells were implanted into the right flanks of 5-week-old male *nu/nu* mice (weight 20.5 g $\pm$ 0.8, mean $\pm$ SEM, $n = 32$). The male *nu/nu* mice were maintained in a specific pathogen-free facility at the University of California at Los Angeles. The animals were randomized into control and treated groups (8 mice per group). Treatment was initiated when the tumors reached a mean diameter of 3 to 4 mm, and the first day of treatment in both cases was designated as day 0. Mice were treated three times weekly with either control vehicle or dasatinib (10 mg/kg) or trametinib (0.5 mg/kg) or a combination of dasatinib and trametinib. Compounds were administered by oral gavage in 80 mmol/L citrate solution with 0.5% hydroxypropylmethyl cellulose and 0.2% Tween-80. Tumor volume (V) was measured with an external caliper and it was calculated as $V = 0.52$ (length $\times$ width^2). All animal experiments in this study were approved by the UCLA Chancellor's Animal Research Committee (protocol no.: 2011-118).

Materials

DMEM, McCoys's medium, FBS, goat anti-mouse IgG secondary antibody conjugated to Alexa Fluor 488 (Thermo Fisher Scientific, Catalog No. A-11029; RRID:AB_2534088). Primary antibodies used were as follows: phospho-FAK Tyr861 (Thermo Fisher Scientific, Catalog No. 44-626-G; RRID:AB_2533703 final dilution 1:1,000); YAP (63.1, Santa Cruz Biotechnology, Catalog No. sc-101199; RRID: AB_1131430, final dilution 1:200), GAPDH (Santa Cruz Biotechnology, Catalog No. sc-365062; RRID:AB_10847862, final dilution 1:500), phospho-YAP Tyr357 (Abcam, Catalog No. ab62751; RRID: AB_956486, final dilution 1:1000); Flag, DYKDDDDK Tag (9A3) Mouse mAb (Cell Signaling Technology, Catalog No. 8146; RRID: AB_10950495, final dilution 1:500), YAP (Cell Signaling Technology, Catalog No. 14074; RRID:AB_2650491 final dilution 1:1,000), phospho ERK1/2 (Thr202/Tyr204, Cell Signaling Technology, Catalog No. 9106; RRID:AB_331768, final dilution 1:1,000), ERK1/2 (Cell Signaling Technology, Catalog No. 4696), phospho-FAK (Tyr576/577, Cell Signaling Technology, Catalog No. 3281; RRID:AB_331079, final dilution 1:1,000), FAK (Cell Signaling Technology, Catalog No. 3285; RRID:AB_2269034, final dilution 1:1000), YES (Cell Signaling Technology, Catalog No. 3201, RRID:AB_11178531, final dilution 1:1,000), Src (Cell Signaling Technology, Catalog No. 2123; RRID: AB_2106047, final dilution 1:1,000) and Src Y416, (Cell Signaling Technology, Catalog No. 6943; RRID:AB_10013641, final dilution 1:1,000). Dasatinib (S1021), Saracatinib (AZD0530, #S1006), PP2 (#S7008), Trametinib (#S1021), and KPT-330 (# S7252) were all from Selleckchem. CH6953755 (HY135299) was from Medchemexpress LLC. All RT-qPCR reagents were obtained from Thermo Fisher Scientific. pcDNA Flag Yap1 (Addgene plasmid; RRID: Addgene_18881) and pcDNA Flag Yap1 Y357F (Addgene plasmid; RRID:Addgene_18882) were gifts from Yosef Shaul; pCMV-flag S127A YAP was a gift from Kunliang Guan (Addgene plasmid; RRID:Addgene_27370). siRNAs were from Santa Cruz Biotechnolgy (Src no. sc-29228 and YES1 no. sc-29860). All other reagents were of the highest grade available.

Statistical analysis

Each experiment was repeated three times independently. Unless otherwise noted, data are presented as mean $\pm$ SEM. Differences in YAP nuclear/cytoplasmic ratios, protein phosphorylation, and colony formation were determined using Student t test and were considered significant if $P < 0.05$. The growth of Mia PaCa-2 cells xenografted in the flank of nude mice was analyzed by ANOVA.

Data availability statement

Data were generated by the authors and included in the article. The data generated in this study are available within the article and its supplementary data files.

Results

Association of SFK expression with unfavorable prognosis and YAP expression in PDAC

As a first step to define the role of SFK members in patients with PDAC, we used an interactive open-access database (www.proteinatlas.org/pathology). We found that higher expression of YES1 is significantly associated with unfavorable prognosis (survival) in PDAC (**Fig. 1A**). Only 7% of the patients with higher levels of YES1 expression survived for 5 years whereas 51% of the subset with the lower levels of YES1 mRNA survived for 5 years or more ($P < 0.001$). Higher expression of Src is also associated with unfavorable prognosis ($P < 0.015$) in PDAC (Supplementary Fig. S1). These findings not only are inconsistent with a tumor suppressive role of SFKs in PDAC but imply that SFKs, especially YES1, are pro-oncogenic. However, the mechanism(s) involved remain poorly understood.

Current evidence indicates that the transcriptional co-activator YAP plays a major role in PDAC development (25, 30, 38, 39). Using the web-based Gene Expression Profiling Analysis (GEPIA) tool (40), we found a strong correlation between YES1 and YAP mRNA expression in PDAC ($R = 0.7$; $P = 1.6e{-}27$; **Fig. 1B**). We also found a statistically significant correlation between Src and YAP mRNA expression in PDAC (Supplementary Fig. S1). The associations of YES and Src with patient survival and YAP expression prompted us to examine the mechanism(s) by which SFKs regulate YAP activity in human PDAC cells.

SFK is rapidly activated in response to stimulation of PDAC cells with neurotensin and insulin

Previously, we demonstrated potent positive crosstalk between insulin/IGF-1 receptors and GPCR signaling systems leading to PDAC cell proliferation (36, 37, 41) but the effect of crosstalk on SFK activity was not determined. To assess SFK activity in intact PDAC cells, we determined the phosphorylation of focal adhesion kinase (FAK) at the activation loop Tyr$^{576/577}$, a sensitive biomarker of SFK activity within intact cells (42, 43). Stimulation of PANC-1 cells with 5 nmol/L neurotensin and 10 ng/mL insulin induced a marked increase in FAK phosphorylation at Tyr$^{576/577}$, which was prominent at the earliest time-point examined (1 min) and persisted for at least 120 minutes (**Fig. 1C**). Treatment with the SFK inhibitor dasatinib (10) abolished basal and stimulated FAK phosphorylation at Tyr$^{576/577}$ (**Fig. 1D**). Saracatinib, a different anilinoquinazoline inhibitor of SFK activity, also inhibited FAK phosphorylation at Tyr$^{576/577}$ in these cells (**Fig. 1D**; Structure of inhibitors in Supplementary Fig. S2). SFK activation in response to agonists was also evident in cells transferred to serum-free medium for 24 hours or not subjected to prior serum starvation (**Fig. 1E**). Stimulation with neurotensin and insulin also induced FAK phosphorylation at Tyr$^{576/577}$ in Mia PaCa-2 cells, an effect prevented by dasatinib or saracatinib treatment (**Fig. 1F**).

Stimulation with neurotensin and insulin also increased FAK phosphorylation at Tyr^{861}, another site phosphorylated by SFKs and

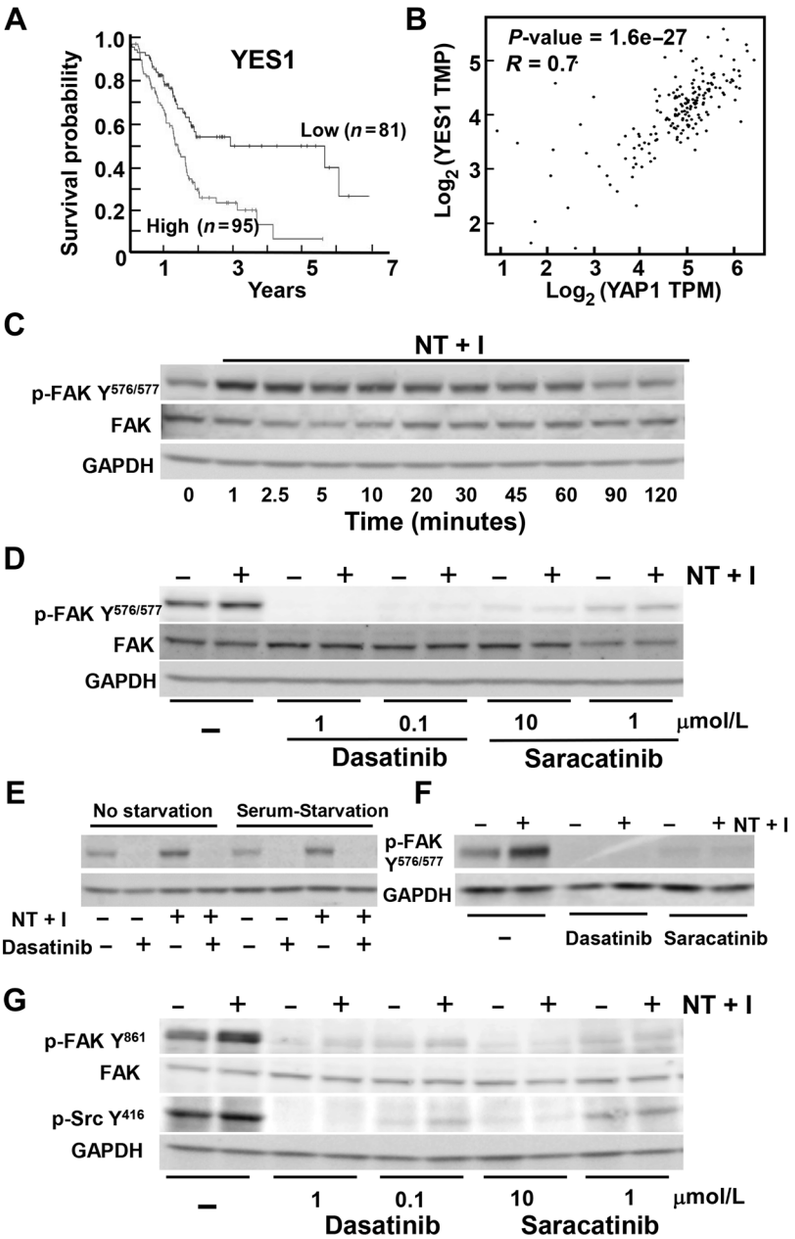

Figure 1.

SFK is associated to PDAC. **A** and **B,** Association of YES1 expression with unfavorable prognosis and YAP expression in PDAC. **C,** SFK is rapidly activated in response to stimulation of intact PDAC cells with neurotensin and insulin. Time-course of FAK $Y^{576/577}$ phosphorylation in PANC-1 cells stimulated with 5 nmol/L neurotensin and 10 ng/mL insulin (NT+I). Immunoblotting of cell lysates was done to determine phosphorylated FAK $Y^{576/577}$, total FAK, and GAPDH. **D,** Dasatinib or saracatinib treatment (1 hour) prevents FAK $Y^{576/577}$ phosphorylation in PANC-1 cells stimulated with NT+I for 1 hour. **E,** FAK $Y^{576/577}$ phosphorylation occurs in serum starved (24 hours) or nonstarved PANC-1 cells. Dasatinib (1 μmol/L) treatment was for 1 hour prior to stimulation with NT+I. **F,** FAK $Y^{576/577}$ phosphorylation in Mia PaCa-2 cells treated with dasatinib (1 μmol/L) or saracatinib (10 μmol/L) for 1 hour prior to stimulation with NT+I. **G,** Dasatinib or saracatinib prevent FAK Y^{861} and Src Y^{416} phosphorylation in PANC-1 cells stimulated with NT+I.

of Src on Tyr^{416}, a key autophosphorylation site in the members of the family (44). Exposure to dasatinib or saracatinib prevented the increase in the phosphorylation of FAK at Tyr^{861} and SFK on Tyr^{416} (**Fig. 1G**). Collectively, the representative Western blots shown in **Fig. 1** indicate that stimulation with neurotensin and insulin elicits rapid SFK activation in PDAC cells.

SFK inhibitors prevent nuclear YAP localization and tyrosine phosphorylation in PDAC cells stimulated with neurotensin and insulin

Next, we determined whether SFK inhibition prevents YAP nuclear import in PDAC cells. Previously, we showed that cell density regulates YAP localization in PANC-1 and Mia PaCa-2. At low cell density, YAP was predominantly localized in the nuclei of these cells, whereas YAP was prominently in the cytoplasm (therefore inactive) of confluent PDAC cells (37, 41). In agreement with previous results (37, 41), stimulation with neurotensin and insulin induced robust YAP nuclear localization in confluent PANC-1 cells. Exposure to dasatinib, saracatinib or PP2, a different SFK inhibitor, blocked the nuclear import of YAP (**Fig. 2A**). Accordingly, SFK inhibitors markedly decreased the expression of the YAP/TEAD-regulated genes *CTGF* and *Cyr61* induced by neurotensin and insulin in PANC-1 cells (Supplementary Fig. S3A). Similarly, SFK inhibitors prevented YAP nuclear import in Mia PaCa-2 (**Fig. 2B**) and Capan 2 cells (Supplementary Fig. S3B). The quantification of the nuclear/cytoplasmic immunofluorescence ratio of YAP in multiple cells is shown in **Fig. 2C** (PANC-1), **Fig. 2D** (Mia PaCa-2), and Supplementary Fig. S3C (Capan 2). These results indicate that the SFKs play a major role in promoting YAP nuclear localization in PDAC cells.

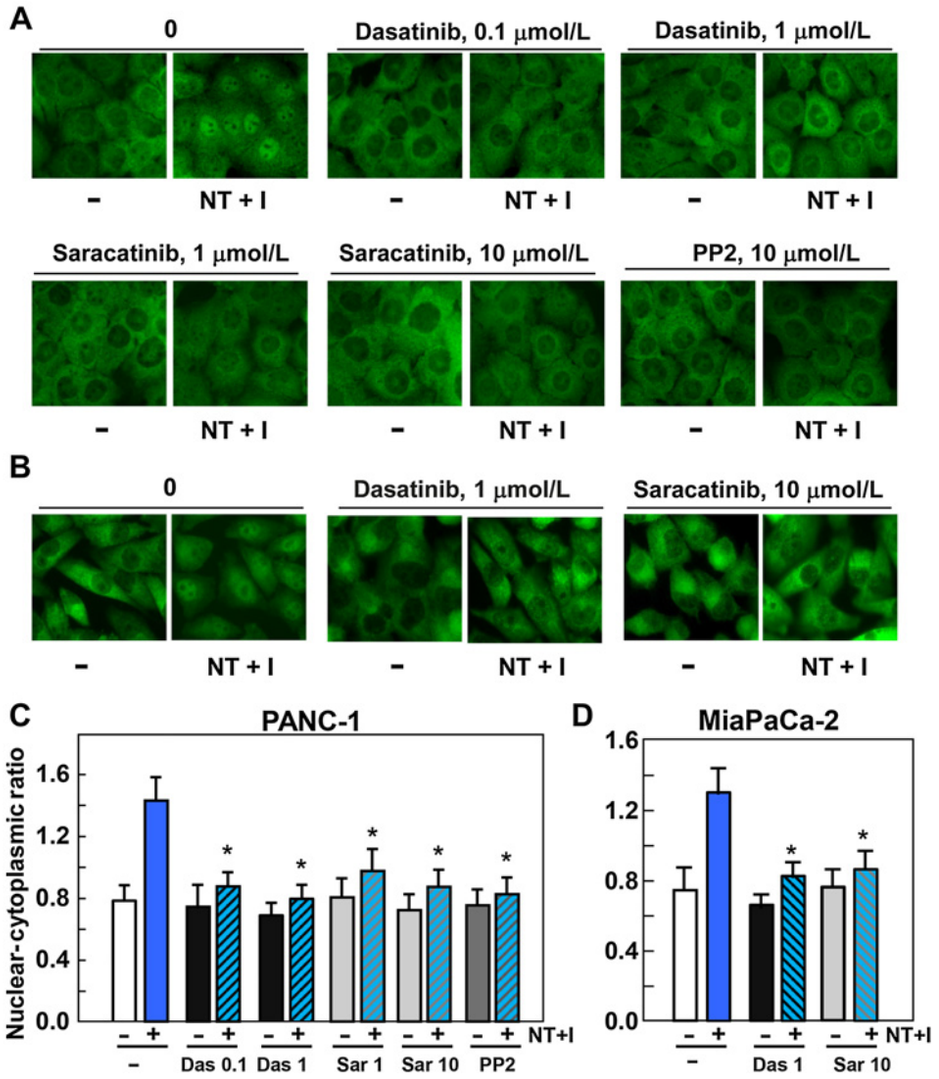

Figure 2.
SFK inhibitors prevent nuclear YAP localization. **A** and **B,** Confluent PANC-1 (**A**) or Mia PaCa-2 (**B**) cells were treated for 1 hour with dasatinib, saracatinib, or PP2 and then stimulated for 1 hour with 5 nmol/L neurotensin and 10 ng/mL insulin (NT+I). The cultures were stained for YAP. **C** and **D,** Bars represent the ratio of nuclear/cytoplasm of YAP in PANC-1 (**C**) or Mia PaCa-2 (**D**). Each bar represents mean ± SEM; $n = 50$ cells, similar reults were obtained in three independent experiments, *t* test *P* values comparing the indicated groups to NT+I were *, $P < 0.01$.

To identify the mechanism(s) by which SFK regulate YAP localization in pancreatic cancer cells, we determined the effect of neurotensin and insulin on YAP tyrosine phosphorylation in PDAC cells. As shown in **Fig. 3A**, stimulation with these agonists induced a marked increase in the phosphorylation of YAP at Tyr^{357} in PANC-1 cells, which was prominent within 10 minutes and persisted for at least 120 minutes. Dasatinib or saracatinib treatment markedly attenuated the increase in YAP phosphorylation at Tyr^{357} (**Fig. 3B**; quantification in **Fig. 3C**). Neurotensin and insulin also induced a time-dependent increase in YAP Tyr^{357} phosphorylation in Mia PaCa-2 cells (Supplementary Fig. S4A). Dasatinib or saracatinib treatment also decreased YAP Tyr^{357} phosphorylation in these cells (Supplementary Fig. S4B). Similar results were obtained with Capan-2 cells (Supplementary Figs. S4C and S4D).

As indicated above, YES1 is the SFK member strongly correlated with unfavorable PDAC prognosis and YAP expression. Recently, the aminopyrazole derivative CH6953755 has been identified as a preferential YES1 tyrosine kinase inhibitor (45). We determined whether this inhibitor also prevents YAP phosphorylation at Tyr^{357} in PDAC cells. Exposure of PANC-1 cells to CH6953755 prior to stimulation with neurotensin and insulin prevented YAP phosphorylation at Tyr^{357} (**Fig. 3D**) and nuclear translocation (Supplementary Fig. S5).

To substantiate the results obtained with chemical inhibitors, we determined whether siRNA-mediated knockdown of YES1 averts YAP phosphorylation at Tyr^{357}. Transient transfection of PANC-1 cells with siRNAs targeting YES1 decreased the level of YES1 protein and prevented the increase in YAP phosphorylation at Tyr^{357} induced by neurotensin and insulin (**Fig. 3E**; quantification in **Fig. 3F**). Collectively, the results show, for the first time, that YES1 plays a major role in mediating YAP phosphorylation on Tyr^{357} and nuclear localization in response to crosstalk between GPCR and insulin receptor signaling pathways in PDAC cells.

Effect of SFK inhibitors on YAP localization and colony-forming ability in low-density cultures of PANC-1 cells

As mentioned above, cell density regulates YAP localization in PANC-1 and Mia PaCa-2. At low cell density, YAP was localized in the nuclei of these cells, whereas YAP was prominently in the cytoplasm of confluent cultures of PDAC cells (37, 41). In agreement with these

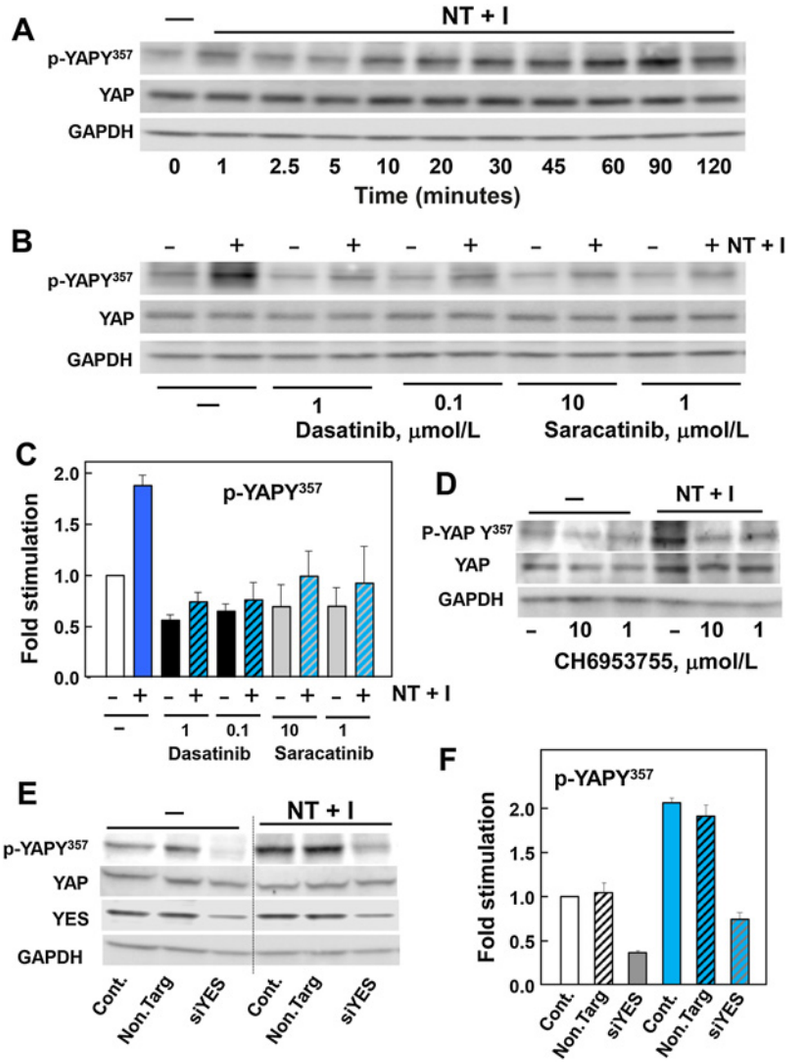

Figure 3.

YAP tyrosine phosphorylation in PANC-1 cells. **A,** Time-course of YAP Y^{357} phosphorylation in response to 5 nmol/L neurotensin and 10 ng/mL insulin (NT+I). Immunoblotting was for phosphorylated YAP Y^{357}, total YAP, and GAPDH. **B,** Dasatinib or saracatinib treatment for 1 hour prevents YAP Y^{357} phosphorylation by NT+I. **C,** Quantification of Western blot signals corresponding to three independent experiments identical to **B**. **D,** CH6953755 inhibits YAP Y^{357} phosphorylation in response to NT+I. **E** and **F,** Effect of siRNA-mediated knockdown of YES1 on YAP Y^{357} phosphorylation in response to NT+I. Irrelevant lanes were spliced out (indicated by a vertical line).

findings, YAP was localized prominently in the nucleus of PANC-1 and Mia PaCa-2 cells growing at low cell densities (**Fig. 4A** and **B**). Dasatinib or saracatinib treatment induced a striking relocalization of YAP from the nucleus to the cytoplasm (**Fig. 4A** and **B**). These results indicate that SFK controls the localization of YAP in low-density, rapidly growing human PDAC cells.

To determine the role of YAP phosphorylation in the regulation of YAP localization in PDAC cells, we used wild type and mutant FLAG-tagged YAP expressed in low-density cultures of PANC-1 cells. As shown with the endogenous YAP, the wild-type FLAG-YAP localized predominantly in the nucleus of low-density PANC-1 cells and redistributed to the cytoplasm in response to dasatinib treatment (**Fig. 4C**). Phosphorylation of Ser^{127} by the LATS1/2 of the Hippo pathway is a recognized mechanism by which YAP is retained in the cytoplasm. Accordingly, expression of FLAG-YAP with Ser^{127} mutated to Ala (FLAG-S127A-YAP) localized in the nucleus. Interestingly, dasatinib treatment induced cytoplasmic localization of FLAG-S127A-YAP, implying that tyrosine phosphorylation overrides regulation through the Hippo pathway (**Fig. 4C**). Crucially, a FLAG-YAP with Tyr^{357} mutated to Phe (FLAG-Y357F-YAP) was excluded from the nucleus of low-density PANC-1 cells, indicating that YAP phosphorylation on Tyr^{357} plays a critical role in controlling YAP localization. Interestingly, FLAG-Y357F-YAP accumulated in the nucleus of cells treated with KPT-330, a potent inhibitor of exportin 1 (XPO-1), the major nuclear-cytoplasmic exportin (**Fig. 4C**). Similar results were obtained when the FLAG-YAP plasmids were transfected to low-density cultures of Mia PaCa-2 cells (**Fig. 4D**). The results indicate that FLAG-Y357F-YAP is not permanently sequestered in the cytoplasm but enters into the nucleus from where it is excluded via XPO-1 and imply that YAP phosphorylation on Tyr^{357} interferes with its nuclear export.

Having established that either SFK inhibitors or mutation of Tyr^{357} to Phe promotes cytoplasmic YAP localization in PANC-1 cells, we next determined whether the SFK inhibitors also inhibit the proliferation of these cells. As shown in **Fig. 4E**, dasatinib inhibited colony formation by PANC-1 cells in a dose-dependent manner.

SFK inhibitors stimulate ERK activity in intact PDAC cells

Although the preceding results suggest that dasatinib could be useful in the treatment of PDAC through inhibition of the SFK/YAP axis, clinical trials in patients with PDAC using dasatinib with

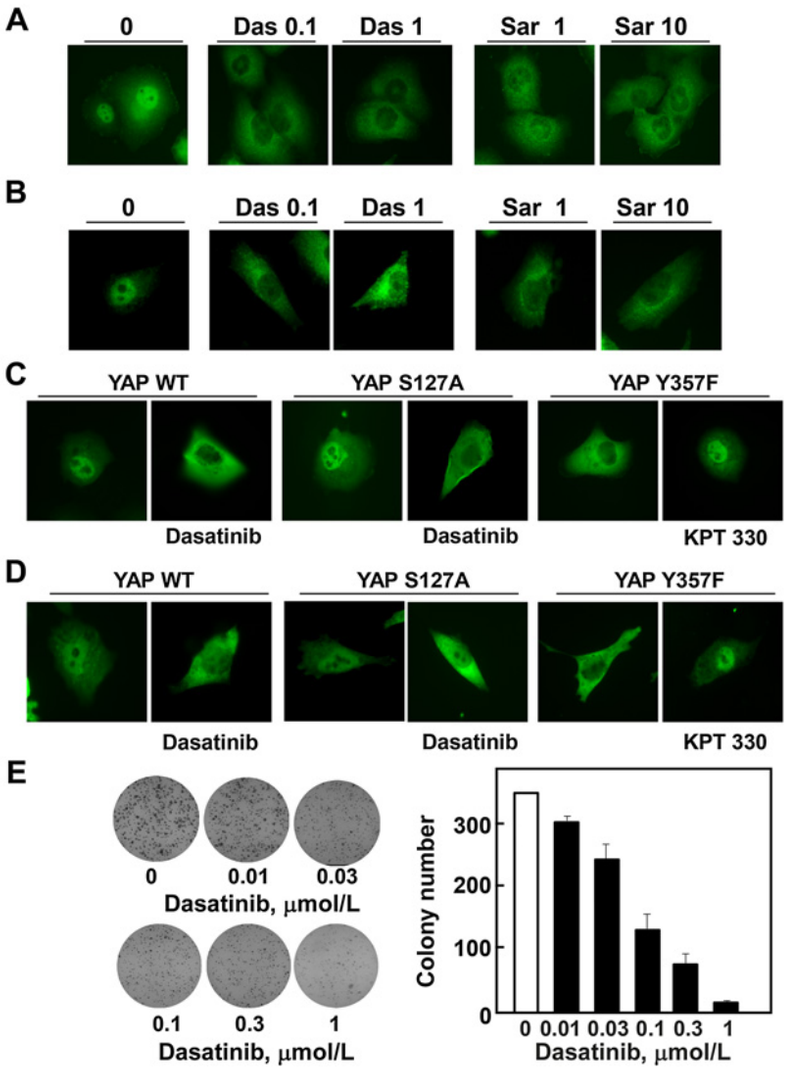

Figure 4.

Role of YAP phosphorylation on localization and colony-forming ability in low-density PDAC cells. **A** and **B,** SFK inhibitors prevent nuclear YAP localization in growing cells. Low-density cultures of PANC-1 (**A**) or Mia PaCa-2 (**B**) cells were treated with dasatinib, or saracatinib at the indicated concentrations for 2 hours and then fixed and stained for YAP. **C** and **D,** YAP Y357F mutation prevents YAP nuclear localization. PANC-1 (**C**) and Mia PaCa-2 (**D**) cells transiently transfected with FLAG epitope-tagged WT or phospho-deficient mutants of YAP (S127A or Y357F). The cultures were then fixed and stained for the FLAG epitope-tag. **E,** Cell colony formation: PANC-1 cells were incubated for 10 days with the indicated concentrations of dasatinib. The bars represent the number of colonies (mean ± SEM; $n = 3$ dishes per condition). Similar results were obtained in three additional experiments.

gemcitabine (12) or 5-fluorouracil and oxaliplatin (14) were unsuccessful. We conjectured that SFK inhibitors not only hinder YAP activation but also activate a compensatory pathway(s) that mediates resistance to these drugs (46). In line with this possibility, we found that treatment with dasatinib induced a marked increase in ERK activity in unstimulated PANC-1 cells or in cells exposed to neurotensin and insulin, as shown by ERK dual phosphorylation on Thr^{202} and Tyr^{204} (**Fig. 5A**; quantification in Supplementary Fig. S6A). Dasatinib-induced ERK activation was completely abolished by exposure to trametinib, a potent MEK inhibitor. Trametinib prevented dasatinib-induced ERK overactivation in PANC-1 cells at a concentration as low as 30 nmol/L (**Fig. 5B**). Saracatinib or PP2 treatment also enhanced ERK activation, and this effect was abrogated by trametinib (**Fig. 5C**). Furthermore, siRNA-mediated knockdown of YES1, SRC, or both decreased their protein levels and promoted ERK overactivation (**Fig. 5D**; quantification in Supplementary Figs. S6B and S6C). Dasatinib or saracatinib treatment markedly increased basal ERK activity in Mia PaCa-2 cells to a level comparable with that produced by agonist stimulation (Supplementary Fig. S6D).

Combination of dasatinib and trametinib synergistically inhibit colony formation by PDAC cells and impairs the growth of Mia PaCa-2 xenografts

Because trametinib prevented dasatinib-induced ERK activation in PDAC cells, we next determined whether trametinib potentiates the inhibitory effect of dasatinib on colony formation by these cells. As illustrated in **Fig. 6A** and **B** dasatinib, at a concentration that has a modest inhibitory effect on colony formation (0.03 μmol/L), markedly potentiated the inhibitory effect of trametinib (0.03 μmol/L). Colony formation by Mia PaCa-2 or Capan 2 cells was drastically inhibited at even lower concentrations. A combination of dasatinib and trametinib each at a concentration as low as 0.003 μmol/L abolished colony formation in either Mia PaCa-2 (**Fig. 6C** and **D**) or Capan 2 cells (Supplementary Fig. S7). The combination index (CI) of dasatinib and trametinib was <1 (i.e., 0.35, 0.4, and 0.38 for PANC-1, Mia Paca-2, and Capan 2, respectively), indicating synergistic interaction between these drugs in inhibiting colony growth in PDAC cell lines. These results show that a combination of dasatinib and trametinib inhibits colony formation of human PDAC cells at clinically relevant concentrations. Furthermore, administration of a combination of dasatinib (10 mg/kg)

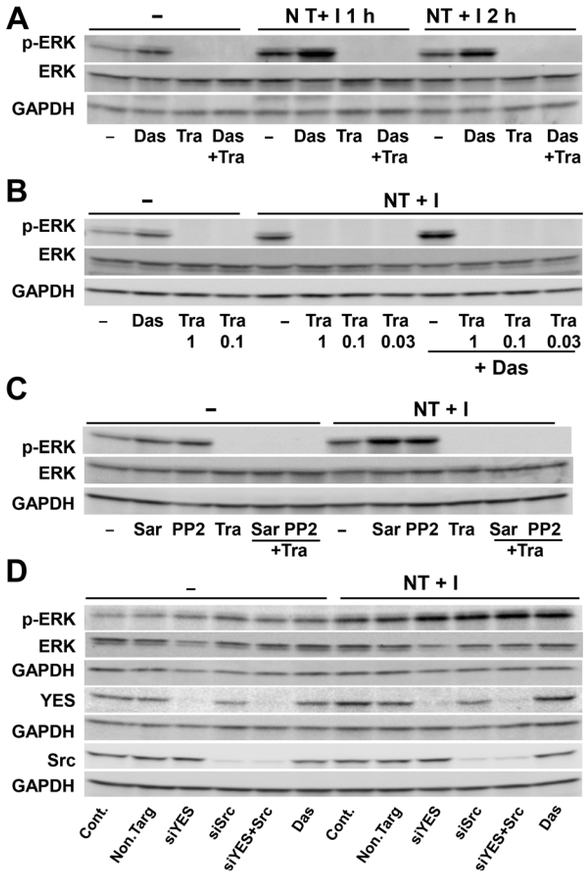

Figure 5.

SFK inhibitors enhance ERK activation in PANC-1 cells: suppression by trametinib. **A,** Confluent PANC-1 cells were treated for 1 hour with 1 μmol/L dasatinib (Das), 1 μmol/L trametinib (Tra), or their combination (Das+Tra) and then stimulated for either 1 or 2 hours with 5 nmol/L neurotensin and 10 ng/mL insulin (NT+Ins). **B,** Cells treated for 1 hour with Das, Tra, or Das+Tra at different concentrations and then stimulated with NT+Ins for 1 hour. **C,** Treatment with saracatinib or PP2 at 10 μmol/L for 1 hour prior to stimulation also enhances ERK activation that is suppressed by Tra. **D,** siRNA-mediated knockdown of YES1, Src, or both enhances ERK activation in response to NT+Ins. Dasatinib (Das) was included for comparison.

and trametinib (0.5 mg/kg) by oral gavage suppressed the growth of Mia PaCa-2 cells xenografted in the flank of nude mice (**Fig. 6E**).

Discussion

PDAC is a highly aggressive disease that is expected to become the second cause of cancer fatalities during the next decade (2). As therapeutic options are limited, novel targets and agents for combinatory therapeutic intervention are urgently required (47). In this context, the highly conserved transcriptional co-activator YAP is attracting intense interest. YAP is a context-specific oncogene (20), which is overactive in PDAC patient tumor samples (26) and associated with poor PDAC survival (25). YAP is highly activated in the squamous subtype of PDAC (30), which exhibits reduced dependency on KRAS for survival (31, 32). Accordingly, overexpression of *Yap* can substitute for mutant *Kras* expression in promoting PDAC in preclinical models (26) and depletion of KRAS protein has minimal effects on the survival of PANC-1 cells (48), a model of squamous subtype of PDAC. Because either YAP or its upstream pathways is rarely mutated in PDAC, the signaling mechanism(s) leading to YAP activation is of critical importance.

Several studies implicated SFK in YAP activation, acting through Hippo-dependent (33, 34) and/or Hippo-independent pathways (35) but the role of SFKs in YAP activation in PDAC cells remained unknown. Here, we show that insulin and the GPCR agonist neurotensin, a potent mitogenic combination, induced rapid SFK activation within intact PANC-1 cells, as judged by FAK phosphorylation at $Tyr^{576/576}$ and Tyr^{861}, sensitive biomarkers of SFK activity within intact cells (42) and Src^{416} autophosphorylation, a critical event in the activation of all members of the SFK (44). Treatment with either dasatinib or saracatinib suppressed SFK activity within PDAC cells. Crucially, these SFK inhibitors blocked YAP nuclear localization stimulated by neurotensin and insulin, implying that SFKs promote YAP nuclear accumulation in human PDAC cells.

SFK have been implicated in the regulation of YAP localization but the mechanisms are cell-context dependent and the role of SFKs in YAP regulation in PDAC cells was not examined before. Here, we show that stimulation of PDAC cells with neurotensin and insulin induced a marked and persistent increase in YAP phosphorylation at Tyr^{357}. Exposure to dasatinib or saracatinib completely prevented the increase in YAP phosphorylation on Tyr^{357}. Furthermore, CH6953755, a preferential YES1 inhibitor (45), also abrogated YAP phosphorylation on Tyr^{357}, suggesting that YES1 plays a major role in mediating YAP phosphorylation in response to agonist stimulation. Accordingly, siRNA-mediated knockdown of YES1 severely impaired YAP phosphorylation on Tyr^{357}. Collectively, these results show, for the first time, that YES1 plays a critical role in promoting YAP tyrosine phosphorylation in PDAC cells. The importance of these mechanistic findings is emphasized by the Kaplan–Meier curves displayed in **Fig. 1**, showing that high YES1 expression is associated with shorter survival of patients with pancreatic cancer.

As mentioned, YAP is localized prominently in the nucleus of PDAC cells growing at low cell densities (37, 41). Dasatinib or saracatinib treatment induced striking relocalization of YAP from the nucleus to the cytoplasm in sparse cultures of PDAC cells. These results suggested that SFK-mediated tyrosine phosphorylation controls the localization of YAP in low-density, rapidly growing human PDAC cells. In line with this notion, a FLAG-YAP with Tyr^{357} mutated to Phe (FLAG-Y357F-YAP) was excluded from the nucleus of PDAC cells. These results substantiate the conclusion that YAP phosphorylation at Tyr^{357} plays a major role in promoting YAP nuclear localization in these cells. Interestingly, FLAG-Y357F-YAP accumulated in the nucleus of cells treated with KPT-330 (49), a potent inhibitor of exportin 1 (XPO-1), the major nuclear-cytoplasmic exportin. The results suggest that FLAG-Y357F-YAP is not irreversibly trapped in the cytoplasm but enters into the nucleus from where it is efficiently excluded via XPO-1. We conclude that YAP phosphorylation at Tyr^{357} reduces the rate of its nuclear export thereby leading to YAP nuclear accumulation.

The preceding results suggest that dasatinib could be useful in the treatment of PDAC through inhibition of the SFK/YAP axis. However, clinical trials in patients with PDAC using dasatinib in combination with gemcitabine (12) or 5-fluorouracil and oxaliplatin (14) were unsuccessful. We considered that SFK inhibitors not only hinder YAP activation but concomitantly trigger activation of a compensatory pathway(s) that mediates resistance to these drugs (46). Accordingly, we found that treatment of PDAC cells with SFK inhibitors increased basal ERK activity and further enhanced ERK activation by mitogenic

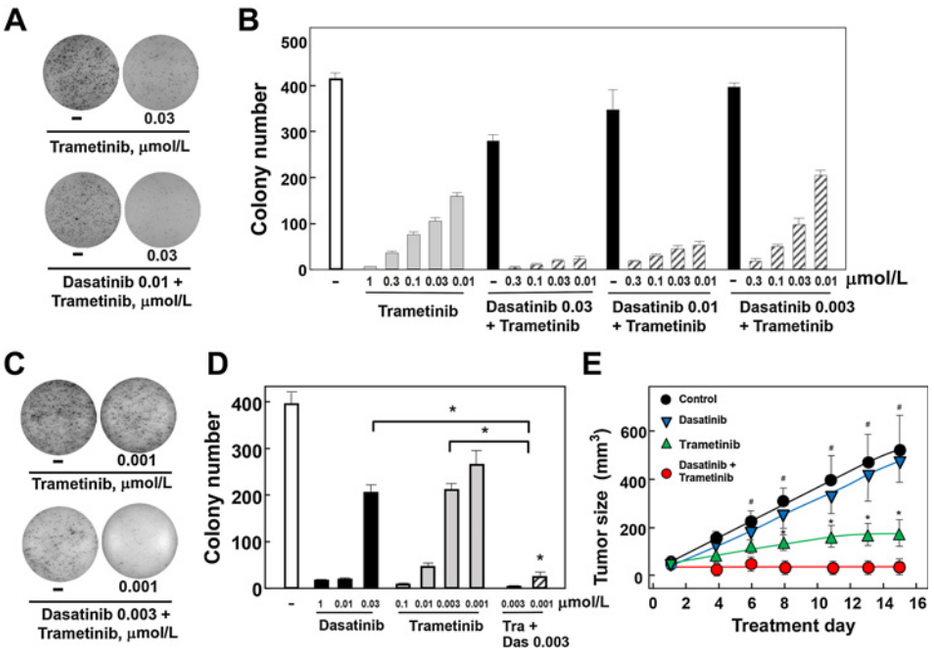

Figure 6.

Combination of dasatinib and trametinib potently inhibit colony formation by PDAC cells. **A** and **C,** Representative plates of PANC-1 (**A**) and Mia PaCa-2 (**C**) treated with either dasatinib, trametinib, or a combination at the concentrations shown. **B** and **D,** The bars represent the number of colonies in PANC-1 (**B**) and Mia PaCa-2 (**D**; mean ± SEM; $n = 3$ dishes per condition). Similar results were obtained in four (PANC-1) and three (Mia PaCa-2) independent experiments. *, *t* test *P* values comparing the indicated two groups were < 0.001. **E,** Administration of dasatinib (10 mg/kg) or trametinib (0.5 mg/kg), or a combination of dasatinib and trametinib by oral gavage (3 doses/week) suppressed the growth of Mia PaCa-2 cells xenografted in the flank of nude mice (8 mice per group). #, $P < 0.001$ (contol vs. dasatinib and trametinib); *, $P < 0.001$ (trametinib vs. dasatinib and trametinib).

agonists. Previous studies showed that dasatinib (50), like RAF inhibitors (51), induced BRAF/CRAF dimerization leading to MEK/ERK activation in a Ras-dependent manner. Dasatinib was thought to act as a weak inhibitor of RAF isoforms leading to paradoxical activation of the pathway (50). Our results do not support this mechanism in PDAC cells because we also observed ERK activation in response to saracatinib, a structurally different SFK inhibitor which does not inhibit BRAF or CRAF, even at high concentrations (52). Importantly, we also show that siRNA-mediated knockdown of Src/YES also induce ERK activation. We therefore conclude that pharmacologic or genetic suppression of SFK activity leads to ERK activation through a mechanism that differs from that used by RAF inhibitors.

Recent studies showed that SFK directly phosphorylates KRAS on Tyr^{32} and Tyr^{64} and inhibits its ability to activate RAF/MEK/ERK (15, 53). Consequently, it is plausible that exposure to SFK inhibitors induces RAS hyper-activation, thereby leading to enhanced RAF/MEK/ERK signaling in PDAC cells by blocking SFK-mediated inhibitory phosphorylation of RAS, a proposition that warrants further experimental work. Our results also demonstrate that SFK-induced ERK activation was completely abolished by cell exposure to the FDA-approved MEK inhibitor trametinib. Importantly, the combination of dasatinib and trametinib, each inhibitor at clinically relevant concentrations, completely blocked YAP phosphorylation on Tyr^{357} and ERK activation and prevented colony growth by PDAC cells in a synergistic manner. Indeed, colony formation by PANC-1, Mia PaCa-2, or Capan 2 was only abolished when both pathways (Src/YAP and MEK/ERK) were inhibited. The dasatinib/trametinib combination also inhibited the growth of Mia PaCa-2 cells xenografted in nude mice. Thus, these results provide a mechanistic rationale to consider that a combination of the FDA-approved inhibitors dasatinib with trametinib should be considered for clinical trials in PDAC. Our study is in agreement with other recent reports that identified empirically the combination of dasatinib and trametinib as a plausible therapeutic intervention for cancers with *KRAS*-activating mutation (54, 55) but differs from these studies because the results presented here provide a mechanistic rationale for the interaction between the inhibitors, namely, dasatinib inhibits YAP tyrosine phosphorylation and nuclear localization and trametinib prevents the compensatory ERK activation induced by SFK inhibition. Our results also support the development of novel SFK/panRAF inhibitors, including CCT3833, which inhibits SFK but does not activate ERK and is being evaluated in an early-phase clinical trial (56). In summary, the findings presented here identify an important interplay between SFKs, YAP and MEK/ERK in PDAC sensitivity to drug combinations and support clinical testing of a combination of FDA-approved SFK and MEK inhibitors in PDAC treatment and the development of novel dual SFK/RAF inhibitors.

Authors' Disclosures

G. Eibl reports grants from NCI during the conduct of the study. No disclosures were reported by the other authors.

Authors' Contributions

J. Sinnet-Smith: Conceptualization, resources, data curation, formal analysis, supervision, funding acquisition, validation, investigation, methodology, writing–original draft, project administration, writing–review and editing. **T. Anwar:** Resources, data curation, formal analysis, funding acquisition, investigation, methodology, writing–review and editing. **E.F. Reed:** Resources, data curation, formal analysis, supervision, funding acquisition, investigation, methodology, project administration, writing–review and editing. **Y. Teper:** Investigation, methodology. **G. Eibl:** Resources, funding acquisition, writing–review and editing. **E. Rozengurt:** Conceptualization, resources, data curation, formal analysis, supervision, funding acquisition, validation, investigation, methodology, writing–original draft, project administration, writing–review and editing.

Acknowledgments

E.F. Reed was supported by grants P01CA236585, R21CA258125, R21AI156592 and Department of Veterans Affair Merit Award 1I01BX003801. E.F. Reed was supported by grants R01 AI135201, U19 AI128913, P01AI120944, R21AI156592, and U01 AI-124319. G. Eibl was supported by grants P01CA236585 and R21CA258125.

Additional funding from the Ronald S. Hirschberg Endowed Chair of Pancreatic Cancer Research to E.F. Reed and a Ronald S. Hirschberg Foundation Grant to G. Eibl.

The publication costs of this article were defrayed in part by the payment of publication fees. Therefore, and solely to indicate this fact, this article is hereby marked "advertisement" in accordance with 18 USC section 1734.

Note

Supplementary data for this article are available at Molecular Cancer Therapeutics Online (http://mct.aacrjournals.org/).

Received December 1, 2021; revised April 22, 2022; accepted August 19, 2022; published first August 23, 2022.

References

1. Siegel RL, Miller KD, Fuchs HE, Jemal A. Cancer statistics, 2021. CA Cancer J Clin 2021;71:7–33.
2. Rahib L, Smith BD, Aizenberg R, Rosenzweig AB, Fleshman JM, Matrisian LM. Projecting cancer incidence and deaths to 2030: the unexpected burden of thyroid, liver, and pancreas cancers in the United States. Cancer Res 2014;74:2913–21.
3. Eibl G, Rozengurt E. KRAS, YAP, and obesity in pancreatic cancer: a signaling network with multiple loops. Semin Cancer Biol 2019;54:50–62.
4. Hingorani SR, Wang L, Multani AS, Combs C, Deramaudt TB, Hruban RH, et al. Trp53R172H and KrasG12D cooperate to promote chromosomal instability and widely metastatic pancreatic ductal adenocarcinoma in mice. Cancer Cell 2005;7:469–83.
5. Collisson EA, Bailey P, Chang DK, Biankin AV. Molecular subtypes of pancreatic cancer. Nat Rev Gastroenterol Hepatol 2019;16:207–20.
6. Moro L, Simoneschi D, Kurz E, Arbini AA, Jang S, Guaragnella N, et al. Epigenetic silencing of the ubiquitin ligase subunit FBXL7 impairs c-SRC degradation and promotes epithelial-to-mesenchymal transition and metastasis. Nat Cell Biol 2020;22:1130–42.
7. Martellucci S, Clementi L, Sabetta S, Mattei V, Botta L, Angelucci A. Src family kinases as therapeutic targets in advanced solid tumors: what we have learned so far. Cancers 2020;12:1448.
8. Nagaraj NS, Smith JJ, Revetta F, Washington MK, Merchant NB. Targeted inhibition of SRC kinase signaling attenuates pancreatic tumorigenesis. Mol Cancer Ther 2010;9:2322–32.
9. Je DW, O YM, Ji YG, Cho Y, Lee DH. The inhibition of src family kinase suppresses pancreatic cancer cell proliferation, migration, and invasion. Pancreas 2014;43:768–76.
10. Araujo J, Logothetis C. Dasatinib: a potent SRC inhibitor in clinical development for the treatment of solid tumors. Cancer Treat Rev 2010;36:492–500.
11. Morton JP, Karim SA, Graham K, Timpson P, Jamieson N, Athineos D, et al. Dasatinib inhibits the development of metastases in a mouse model of pancreatic ductal adenocarcinoma. Gastroenterology 2010;139:292–303.
12. Mettu NB, Niedzwiecki D, Rushing C, Nixon AB, Jia J, Haley S, et al. A phase I study of gemcitabine + dasatinib (gd) or gemcitabine + dasatinib + cetuximab (GDC) in refractory solid tumors. Cancer Chemother Pharmacol 2019;83:1025–35.
13. Evans TRJ, Van Cutsem E, Moore MJ, Bazin IS, Rosemurgy A, Bodoky G, et al. Phase 2 placebo-controlled, double-blind trial of dasatinib added to gemcitabine for patients with locally-advanced pancreatic cancer. Ann Oncol 2017;28:354–61.
14. George TJ, Ali A, Wang Y, Lee JH, Ivey AM, DeRemer D, et al. Phase II study of 5-fluorouracil, oxaliplatin plus dasatinib (FOLFOX-D) in first-line metastatic pancreatic adenocarcinoma. Oncologist 2021;26:825–e1674.
15. Kano Y, Gebregiworgis T, Marshall CB, Radulovich N, Poon BPK, St-Germain J, et al. Tyrosyl phosphorylation of KRAS stalls GTPase cycle via alteration of switch I and II conformation. Nat Commun 2019;10:224.
16. Buday L, Vas V. Novel regulation of Ras proteins by direct tyrosine phosphorylation and dephosphorylation. Cancer Metastasis Rev 2020;39:1067–73.
17. Nichols RJ, Haderk F, Stahlhut C, Schulze CJ, Hemmati G, Wildes D, et al. RAS nucleotide cycling underlies the SHP2 phosphatase dependence of mutant BRAF-, NF1- and RAS-driven cancers. Nat Cell Biol 2018;20:1064–73.
18. Ruess DA, Heynen GJ, Ciecielski KJ, Ai J, Berninger A, Kabacaoglu D, et al. Mutant KRAS-driven cancers depend on PTPN11/SHP2 phosphatase. Nat Med 2018;24:954–60.
19. Bunda S, Burrell K, Heir P, Zeng L, Alamsahebpour A, Kano Y, et al. Inhibition of SHP2-mediated dephosphorylation of Ras suppresses oncogenesis. Nat Commun 2015;6:8859.
20. Moroishi T, Hansen CG, Guan K-L. The emerging roles of YAP and TAZ in cancer. Nat Rev Cancer 2015;15:73–9.
21. Meng Z, Moroishi T, Guan K-L. Mechanisms of Hippo pathway regulation. Genes Dev 2016;30:1–17.
22. Totaro A, Panciera T, Piccolo S. YAP/TAZ upstream signals and downstream responses. Nat Cell Biol 2018;20:888–99.
23. Zhang W, Nandakumar N, Shi Y, Manzano M, Smith A, Graham G, et al. Downstream of mutant KRAS, the transcription regulator YAP is essential for neoplastic progression to pancreatic ductal adenocarcinoma. Sci Signal 2014;7:ra42–ra.
24. Gruber R, Panayiotou R, Nye E, Spencer-Dene B, Stamp G, Behrens A. YAP1 and TAZ control pancreatic cancer initiation in mice by direct up-regulation of JAK–STAT3 signaling. Gastroenterology 2016;151:526–39.
25. Rozengurt E, Sinnett-Smith J, Eibl G. Yes-associated protein (YAP) in pancreatic cancer: at the epicenter of a targetable signaling network associated with patient survival. Signal Transduct Targeted Ther 2018;3:11.
26. Kapoor A, Yao W, Ying H, Hua S, Liewen A, Wang Q, et al. Yap1 activation enables bypass of oncogenic kras addiction in pancreatic cancer. Cell 2014;158:185–97.
27. Morvaridi S, Dhall D, Greene MI, Pandol SJ, Wang Q. Role of YAP and TAZ in pancreatic ductal adenocarcinoma and in stellate cells associated with cancer and chronic pancreatitis. Sci Rep 2015;5:16759.
28. Yang S, Zhang L, Purohit V, Shukla SK, Chen X, Yu F, et al. Active YAP promotes pancreatic cancer cell motility, invasion and tumorigenesis in a mitotic phosphorylation-dependent manner through LPAR3. Oncotarget 2015;6:36019–31.
29. Murakami S, Shahbazian D, Surana R, Zhang W, Chen H, Graham GT, et al. Yes-associated protein mediates immune reprogramming in pancreatic ductal adenocarcinoma. Oncogene 2017;36:1232–44.
30. Tu B, Yao J, Ferri-Borgogno S, Zhao J, Chen S, Wang Q, et al. YAP1 oncogene is a context-specific driver for pancreatic ductal adenocarcinoma. JCI Insight 2019;4:e130811.
31. Muzumdar MD, Chen PY, Dorans KJ, Chung KM, Bhutkar A, Hong E, et al. Survival of pancreatic cancer cells lacking KRAS function. Nat Commun 2017;8:1090.
32. Collisson EA, Sadanandam A, Olson P, Gibb WJ, Truitt M, Gu S, et al. Subtypes of pancreatic ductal adenocarcinoma and their differing responses to therapy. Nat Med 2011;17:500–3.
33. Si Y, Ji X, Cao X, Dai X, Xu L, Zhao H, et al. Src inhibits the hippo tumor suppressor pathway through tyrosine phosphorylation of Lats1. Cancer Res 2017;77:4868–80.
34. Lamar JM, Xiao Y, Norton E, Jiang Z-G, Gerhard GM, Kooner S, et al. SRC tyrosine kinase activates the YAP/TAZ axis and thereby drives tumor growth and metastasis. J Biol Chem 2019;294:2302–17.
35. Rosenbluh J, Nijhawan D, Cox AG, Li X, Neal JT, Schafer EJ, et al. β-catenin driven cancers require a YAP1 transcriptional complex for survival and tumorigenesis. Cell 2012;151:1457–73.
36. Kisfalvi K, Eibl G, Sinnett-Smith J, Rozengurt E. Metformin disrupts crosstalk between G protein-coupled receptor and insulin receptor signaling systems and inhibits pancreatic cancer growth. Cancer Res 2009;69:6539–45.
37. Hao F, Xu Q, Zhao Y, Stevens JV, Young SH, Sinnett-Smith J, et al. Insulin receptor and GPCR crosstalk stimulates YAP via PI3K and PKD in pancreatic cancer cells. Mol Cancer Res 2017;15:929–41.
38. Rozengurt E, Eibl G. Central role of Yes-associated protein and WW-domain-containing transcriptional co-activator with PDZ-binding motif in pancreatic cancer development. World J Gastroenterol 2019;25:1797–816.
39. Park J, Eisenbarth D, Choi W, Kim H, Choi C, Lee D, et al. YAP and AP-1 cooperate to initiate pancreatic cancer development from ductal cells in mice. Cancer Res 2020;80:4768–79.
40. Tang Z, Li C, Kang B, Gao G, Li C, Zhang Z. GEPIA: a web server for cancer and normal gene expression profiling and interactive analyses. Nucleic Acids Res 2017;45:W98–W102.

41. Hao F, Xu Q, Wang J, Yu S, Chang H-H, Sinnett-Smith J, et al. Lipophilic statins inhibit YAP nuclear localization, co-activator activity and colony formation in pancreatic cancer cells and prevent the initial stages of pancreatic ductal adenocarcinoma in KrasG12D mice. PLoS One 2019;14: e0216603.
42. Ciccimaro E, Hanks SK, Blair IA. Quantification of focal adhesion kinase activation loop phosphorylation as a biomarker of Src activity. Mol Pharmacol 2009;75:658–66.
43. Lee BY, Timpson P, Horvath LG, Daly RJ. FAK signaling in human cancer as a target for therapeutics. Pharmacol Ther 2015;146:132–49.
44. Roskoski R. Src protein-tyrosine kinase structure, mechanism, and small molecule inhibitors. Pharmacol Res 2015;94:9–25.
45. Hamanaka N, Nakanishi Y, Mizuno T, Horiguchi-Takei K, Akiyama N, Tanimura H, et al. YES1 is a targetable oncogene in cancers harboring *YES1* gene amplification. Cancer Res 2019;79:5734–45.
46. Rozengurt E, Soares HP, Sinnet-Smith J. Suppression of feedback loops mediated by PI3K/mTOR induces multiple overactivation of compensatory pathways: an unintended consequence leading to drug resistance. Mol Cancer Ther 2014;13: 2477–88.
47. Wang S, Zheng Y, Yang F, Zhu L, Zhu X-Q, Wang Z-F, et al. The molecular biology of pancreatic adenocarcinoma: translational challenges and clinical perspectives. Signal Transduct Target Ther 2021;6:249.
48. Singh A, Greninger P, Rhodes D, Koopman L, Violette S, Bardeesy N, et al. A gene expression signature associated with "K-Ras addiction" reveals regulators of EMT and tumor cell survival. Cancer Cell 2009;15:489–500.
49. Sun Q, Carrasco YP, Hu Y, Guo X, Mirzaei H, Macmillan J, et al. Nuclear export inhibition through covalent conjugation and hydrolysis of Leptomycin B by CRM1. Proc Natl Acad Sci U S A 2013;110:1303–8.
50. Packer LM, Rana S, Hayward R, O'Hare T, Eide CA, Rebocho A, et al. Nilotinib and MEK inhibitors induce synthetic lethality through paradoxical activation of RAF in drug-resistant chronic myeloid leukemia. Cancer Cell 2011;20:715–27.
51. Hatzivassiliou G, Song K, Yen I, Brandhuber BJ, Anderson DJ, Alvarado R, et al. RAF inhibitors prime wild-type RAF to activate the MAPK pathway and enhance growth. Nature 2010;464:431–5.
52. Williams E, Bagarova J, Kerr G, Xia D-D, Place ES, Dey D, et al. Saracatinib is an efficacious clinical candidate for fibrodysplasia ossificans progressiva. JCI Insight 2021;6:e95042.
53. Huang Z, Liu M, Li D, Tan Y, Zhang R, Xia Z, et al. PTPN2 regulates the activation of KRAS and plays a critical role in proliferation and survival of KRAS-driven cancer cells. J Biol Chem 2020;295:18343–54.
54. Witkiewicz AK, Balaji U, Eslinger C, McMillan E, Conway W, Posner B, et al. Integrated patient-derived models delineate individualized therapeutic vulnerabilities of pancreatic cancer. Cell Rep 2016;16:2017–31.
55. Rao G, K I-k, Conforti F, Liu J, Zhang Y-W, Giaccone G. Dasatinib sensitises KRAS-mutant cancer cells to mitogen-activated protein kinase kinase inhibitor via inhibition of TAZ activity. Eur J Cancer 2018;99:37–48.
56. Saturno G, Lopes F, Niculescu-Duvaz I, Niculescu-Duvaz D, Zambon A, Davies L, et al. The paradox-breaking panRAF plus SRC family kinase inhibitor, CCT3833, is effective in mutant KRAS-driven cancers. Ann Oncol 2021;32: 269–78.